GEOPHYSICS, VOL. 59, NO. 10 (OCTOBER 1994); P. 1561–1569, 6 FIGS.

Pulse distortion in depth migration

Martin Tygel*, Jörg Schleicher‡, and Peter Hubral‡

ABSTRACT

When migrating seismic primary reflections obtained from arbitrary source-receiver configurations (e.g., common shot or constant offset) into depth, a pulse distortion occurs along the reflector. This distortion exists even if the migration was performed using the correct velocity model. Regardless of the migration algorithm, this distortion is a consequence of varying reflection angle, reflector dip, and/or velocity variation. The relationship between the original time pulse and the depth pulse after migration can be explained and quantified in terms of a prestack, Kirchhoff-type, diffraction-stack migration theory.

INTRODUCTION

Seismic primary reflections obtained from arbitrary source-receiver configurations (e.g., common shot or constant offset) are recorded as seismic wavelets that have a certain duration. Figure 1 shows a sketch of a smooth subsurface reflector below an inhomogeneous velocity overburden. Like all other figures in this paper, Figure 1 shows a 2-D sketch of a 3-D situation. Note, however, that all formulas that will be presented are generally valid in both 2-D and 3-D situations. Suppose that a seismic experiment was performed with different source and receiver positions $S(\xi)$ and $G(\xi)$ as specified by the 2-D parameter vector ξ (Bleistein, 1987; Schleicher et al., 1993). According to ray theory and under the assumption of reproducible sources and receivers, as well as subcritical incidence, a reflection event is described (apart from slowly changing amplitude factors) by identical reflected causal pulses of equal length L in time (i.e., scaled copies of the causal source pulse) at all receivers. For a discussion on how the length of a wavelet can be defined and how it can be determined from the seismic data see, e.g., Berkhout (1984). Thus, all reflections fall into a strip (i.e., the reflector image) of constant width in time with the reflection traveltime surface $\tau_R(\xi)$ as the lower boundary. For noncausal pulses, the true reflection time surface lies somewhere within the strip.

When migrated to depth using any standard migration scheme, the reflector image assumes a certain "thickness" in the form of the depth-migrated strip. For causal wavelets, the reflector is the upper boundary of the depth-migrated strip. For noncausal pulses, it is located somewhere within the strip. It is important to note that the thickness of this strip will, in general, vary along the reflector. For that reason, interpreters may fail to correctly locate the reflector even when using the correct velocity model, when they rely on the wavelet's maximum only, because the distance of the wavelet maximum to the true reflector location varies with the length of the migrated wavelet. In what follows, we call a reflector any smooth subsurface interface that would result from a map migration of the reflection traveltime surface $\tau_R(\xi)$, irrespective of whether the velocity model is correct or not. In other words, the considerations and formulas presented here are valid for correct and incorrect macro-velocity models as well.

Why a laterally varying depth-migrated strip is obtained can be explained easily by simple geometrical considerations. Consider the points along the reflection traveltime surface $\tau_R(\xi)$ (Figure 2, bold traveltime curve). For each of these points, there exists one isochrone surface (or aplanat) in the subsurface that is, for a given macro-velocity model, entirely defined by the source and receiver positions and the observed reflection time. This surface is the locus of all subsurface points that have the property that the sum of the traveltimes along the two ray branches connecting the selected subsurface point to both the shot and receiver equals the given reflection time. The envelope of all isochrones thus specifies the reflector (bold curve). Now consider the points along the parallel traveltime surface $\tau_R(\xi) + L$ (dashed traveltime curve in Figure 2). These points also define a set of isochrones, the envelope of which is the lower boundary of the depth-migrated strip of the reflection (dashed curve). The thickness of the latter strip naturally depends on L, the

Manuscript received by the Editor July 13, 1993; revised manuscript received March 15, 1994.
*Department Matematica Aplicada, University Est. de Campinas (UNICAMP), C.P. 6065, 13081-970 Campinas, S.P., Brazil.
‡Geophysical Institute, Karlsruhe University, Hertzstrasse 16, Geb. 42, 76187 Karlsruhe, Germany.

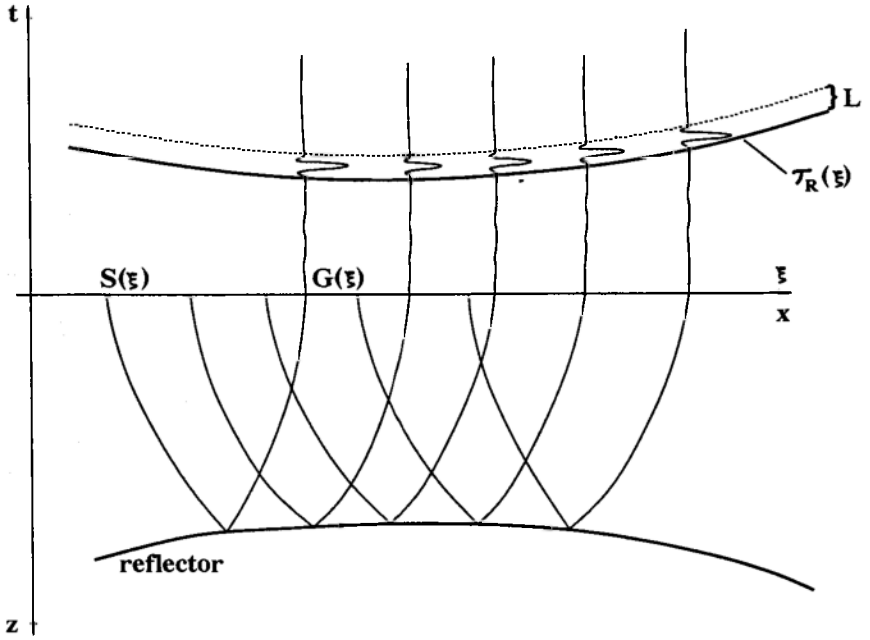

FIG. 1. 2-D sketch of seismic reflections in the (t, ξ) domain. These reflections are created at a curved reflector below a laterally inhomogeneous velocity overburden by an arbitrary seismic recording configuration. Moving sources $S(\xi)$ and receivers $G(\xi)$ are defined by a common parameter vector ξ. Because of the length L of the real (causal) seismic source wavelet, the reflector is mapped onto a strip of constant width L along the time axis, with the correct reflection traveltime surface $\tau_R(\xi)$ being the lower boundary.

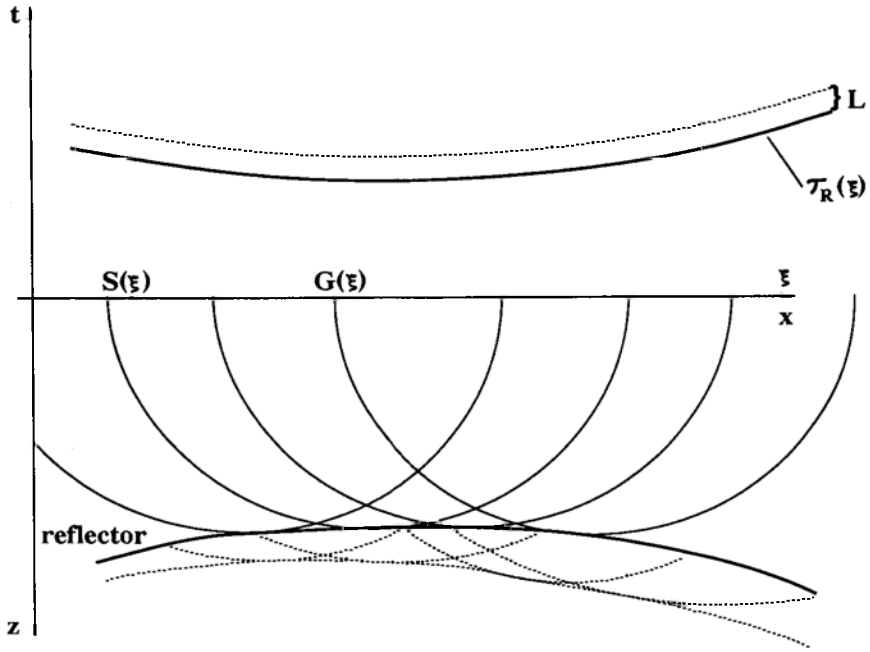

FIG. 2. 2-D sketch of a map migration. For each point on the reflection time surface $\tau_R(\xi)$, there exists one isochrone surface (or aplanat). The envelope of all of these points defines the reflector location (bold curve). The same construction holds for the upper boundary of the mapped strip $\tau_R(\xi) + L$. The result is a depth-migrated strip, the width of which varies along the reflector.

local velocity, the depth of the reflector, and on the seismic measurement configuration.

In this paper, we provide an approximate expression for the 3-D depth-migrated image at a point M vertically below, but still in the near vicinity of, a point M_R located on the reflector (Figure 3a). In other words, we derive a formula that quantitatively describes not only the above indicated pulse distortion, but also gives an expression for the amplitude of the migrated wavelet. Note that any deviation of the ray-theoretical assumption of a constant wavelet length L in the seismic section results in an additional distortion that is not described by the present approach.

Let us now comment on why we define the wavelet distortion in the vertical direction. Of course, if a certain part of a seismic record trace contributes to the migrated image of the desired reflector in the sense of a specular reflection, then the immediate time neighborhood of that part from the same trace will also be migrated to a neighborhood of the previous image. The new image location is generally not vertically below the first image. The direction in which the image location is displaced depends on a number of factors including the time dip, the velocity distribution, and the particular type of trace gather which is being migrated. This is, however, not the direction in which the migrated seismic pulse appears because of seismic trace plotting conventions. Because the migrated seismic traces are typically displayed in the direction of the vertical axis, the distortion is most naturally observed along the same direction.

GEOMETRICAL APPROACH

The stretching factor m_0 for a wavelet $w(t)$ when migrated from time to depth can be derived by simple geometrical arguments in a heuristical way. Although the result can be proven only from the more rigorous mathematical examination that is given below, it is useful to attach a geometrical meaning to the stretching factor so as to make it more plausible. For that purpose, we consider the fixed depth point M_R with coordinates (x_0, y_0, z_0) in Figure 3a together with its diffraction time surface $\tau_D(M_R; \xi)$. The point M_R is located at a reflector, that is fixed throughout the analysis. However, this reflector is assumed to not be specified in the macro-velocity model; i.e., the velocity is taken to be continuous at M_R. If this is not the case, different values for the stretching factor are obtained on either side of the interface.

When the depth point M_R is vertically displaced to a point M with coordinates (x_0, y_0, z), its diffraction time surface $\tau_D(M; \xi)$ is shifted in time by an amount $\Delta\tau = \tau_D(M; \xi) - \tau_D(M_R; \xi)$. The vertical distance $\Delta z = z - z_0$ between M_R and M (Figure 3b) is considered to be small. The traveltime difference between the two rays from S to M (ray SM) and from S to M_R (ray SM_R) is then obtained by the difference between the length of these rays, $\Delta z \cos \Theta_{M_R}$, divided by the local velocity v_{M_R} at M_R. Correspondingly, the difference in travel distance between the two rays connecting M_R to G (ray M_RG) and M to G (ray MG) is $\Delta z \cos \Theta^{+}_{M_R}$. Therefore, along each of the two ray branches associated with M we have the additional traveltime $\Delta z \cos \Theta^{\pm}_{M_R}/v_{M_R}$. For the change of the traveltime when displacing the depth point from M_R to M, we find therefore

$$\Delta\tau = \frac{1}{v_{M_R}} [\cos \Theta^{-}_{M_R} + \cos \Theta^{+}_{M_R}] \Delta z. \tag{1}$$

Why does equation (1) determine the stretching factor? Because, under the assumption that the shape of the wavelet is correctly recovered in the depth-migrated section, it is exactly the local ratio between a small interval $\Delta\tau$ measured in the seismic time section (i.e., the length of the reflected pulse) and a small interval Δz in the seismic depth section (i.e., the length of the depth-migrated pulse) that defines the stretching factor. Therefore, the ratio $\Delta\tau/\Delta z$ equals m_0.

The above considerations provide a geometrical derivation for the stretching factor m_0. We have implicitly assumed that the value resulting from the diffraction stack at M; i.e., the migration result, recovers a scaled and stretched version $Aw(m_0(z - z_0))$ of the source wavelet $w(t)$ and not of another pulse. To verify that this is actually the case, we must now investigate in more detail how the strip in the time record is mapped into the depth domain by the diffraction-stack integral. We will show that a Kirchhoff-type diffraction-stack migration [with arbitrary weights applied to the seismic data along the diffraction traveltime surface $\tau_D(M; \xi)$] indeed reconstructs a scaled version of the source pulse, distorted by the above heuristically derived stretching factor m_0. Unlike the simple kinematic treatment performed above, the following proof is also valid for the more general and realistic cases of overcritical reflections and in the presence of caustics in the wavefield. These cause the reflector image to not only include scaled copies of the source pulse, but also pulses with a certain phase shift. The reason is that in the subsequent analysis, the analytic pulse $W(t)$, consisting of the original (real) source wavelet $w(t)$ as the real part and its Hilbert transform as the imaginary part, is used instead of the real source wavelet $w(t)$ itself.

MATHEMATICAL DERIVATION

In this section, we asymptotically evaluate the Kirchhoff-type diffraction stack at point M with coordinates (x_0, y_0, z) in the near vicinity of the specular reflection point M_R with coordinates (x_0, y_0, z_0) located on the reflector. This result will not only provide the desired expression for the stretching factor m_0, but it will also prove that the migration result at M is indeed the scaled and distorted analytic source wavelet $\Lambda W(m_0(z - z_0))$. An expression for the amplitude factor Λ will also be derived.

As the starting point, we consider the diffraction-stack integral

$$V(M) = \frac{-1}{2\pi} \int\int_A d^2\xi \; w(M; \xi) \left. \frac{\partial U(\xi, t)}{\partial t} \right|_{t = \tau_D(M;\xi)}, \tag{2}$$

where A is the migration aperture, $w(M; \xi)$ is the weight factor, and $U(\xi, t)$ is the analytic seismic trace recorded at the receiver $G(\xi)$ because of a shot at $S(\xi)$. The output $V(M)$ is the value of the depth-migrated image at M. For further information, see Schleicher et al. (1993). Let the analytic reflection seismogram $U(\xi, t)$ in the vicinity of the reflection traveltime surface $\tau_R(\xi)$ contain a P-P reflection event that

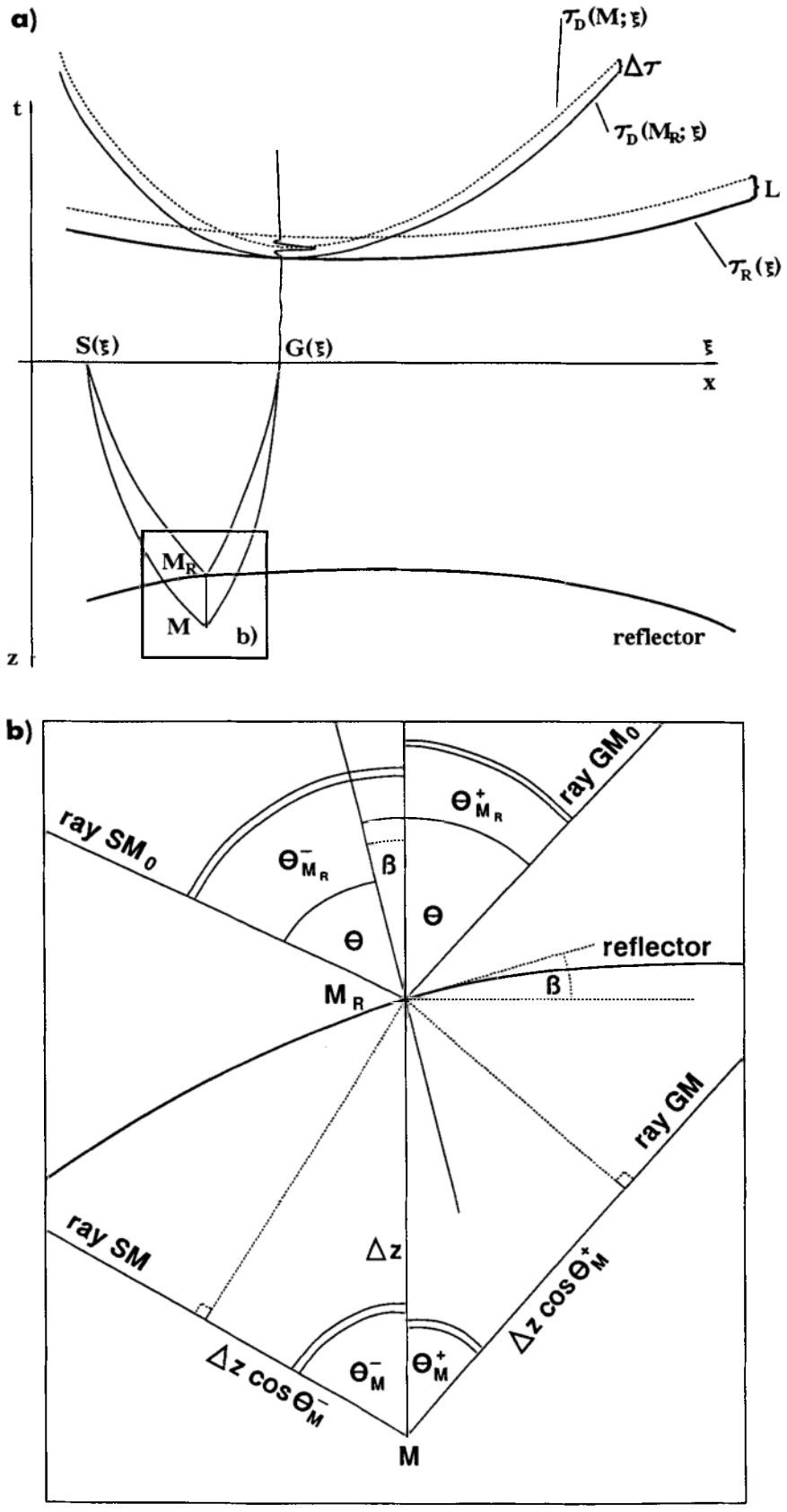

FIG. 3. (a) 2-D sketch of a Kirchhoff-type diffraction stack depth migration. When displacing the chosen depth point $M(x_0, y_0, z)$ vertically from an actual reflection point $M_R(x_0, y_0, z_0)$, the resulting diffraction time surface $\tau_D(M; \xi)$ is shifted in time by a certain amount $\Delta\tau$. (b) Detailed view of a portion of Figure 3a. Shown is a geometrical construction with details on the rays and angles near point M_R.

may be represented in zero-order ray-theoretical description as

$$U(\xi, t) = R_c(\xi)\mathcal{A}(\xi)W(t - \tau_R(\xi))/\mathcal{L}(\xi). \quad (3)$$

The amplitude is given by the product of the (possibly complex) reflection coefficient R_c and the transmission loss $\mathcal{A}$ (which is always real, as long as no evanescent waves are considered) divided by the (either real or imaginary) geometrical-spreading factor $\mathcal{L}$. Introducing expression (3) into equation (2) provides

$$V(M) = \frac{-1}{2\pi} \int\int_A d^2\xi\, w(M; \xi) R_c \times \frac{\mathcal{A}}{\mathcal{L}} \dot{W}(t + [\tau_D(M; \xi) - \tau_R(\xi)]) \Big|_{t=0}, \quad (4)$$

where the dot denotes the time derivative operation. For convenience, we also introduce the notations

$$B(M; \xi) = w(M; \xi)R_c(\xi)\mathcal{A}(\xi)/\mathcal{L}(\xi) \quad (5a)$$

and

$$\tau_F(M; \xi) = \tau_D(M; \xi) - \tau_R(\xi), \quad (5b)$$

from which we recast the diffraction-stack integral in the form

$$V(M) = \frac{-1}{2\pi} \int\int_A d^2\xi\, B(M; \xi)\dot{W}(t + \tau_F(M; \xi)) \Big|_{t=0}. \quad (6)$$

To asymptotically evaluate this integral, we let the time t vary so as to use the Fourier transform. In other words, we consider the time-dependent stack

$$V_1(M; t) = \frac{-1}{2\pi} \int\int_A d^2\xi\, B(M; \xi)\dot{W}(t + \tau_F(M; \xi)), \quad (7)$$

so that the searched-for diffraction-stack migration result is given by

$$V(M) = V_1(M; 0). \quad (8)$$

Applying the Fourier transform with respect to t to equation (7), we obtain, after familiar rules,

$$\hat{V}_1(M; \omega) = \hat{W}(\omega) \frac{i\omega}{2\pi} \int\int_A d^2\xi\, B(M; \xi) e^{i\omega\tau_F(M;\xi)}, \quad (9)$$

in which

$$\hat{V}_1(M; \omega) = \int_{-\infty}^{\infty} dt\, e^{-i\omega t} V_1(M; t) \quad (10a)$$

and

$$\hat{W}(\omega) = \int_{-\infty}^{\infty} dt\, e^{-i\omega t} W(t). \quad (10b)$$

Approximation of $\hat{V}_1(M; \omega)$ in the vicinity of M_R

Let us now make use of the fact that M has the coordinates (x_0, y_0, z); i.e., only the z-coordinate varies from M_R to M (Figure 3a and 3b). Applying a Taylor expansion of $\hat{V}_1(M; \omega)$ in z in the vicinity of z_0, we find for the first-order approximation,

$$\hat{V}_1(M; \omega) \sim \hat{V}_1(M_R; \omega) + \frac{\partial \hat{V}_1}{\partial z}(M_R; \omega)(z - z_0). \quad (11)$$

The first term in equation (11) represents the diffraction-stack integral (9) at M_R on the reflector. As shown in Schleicher et al. (1993), this integral can be asymptotically evaluated upon the use of the method of stationary phase (Bleistein, 1984). Its result is approximated by

$$\hat{V}_1(M_R; \omega) \simeq \hat{W}(\omega)\Lambda(M_R; \xi^*), \quad (12)$$

where ξ^* denotes the stationary or critical point; i.e., the point for which

$$\tau_F(M_R; \xi^*) = 0; \quad (13a)$$

$$\nabla_\xi \tau_F(M_R; \xi)|_{\xi=\xi^*} = \mathbf{0}. \quad (13b)$$

We remark that equation (13b) is the only necessary condition for a stationary point. However, for points M_R, contributions to integral (g) stem only from such points ξ^* where both conditions (13) are fulfilled. Equations (13) describe the fact that the traveltime surfaces $\tau_R(\xi)$ and $\tau_D(M; \xi)$ are tangent as ξ^*. We assume that one and only one critical point ξ^* exists in the aperture range A which satisfies equations (13). If no critical point ξ^* exists in A, the diffraction-stack output will be asymptotically small. On the other hand, if more than one critical point exists in A, the stack result will be a sum of the contributions from each single one. These contributions will show, in general, different amplitudes and different distortions. Therefore, the migrated pulse is no longer under control. However, for most of the usual seismic measurement configurations (e.g., common shot or constant offset), the latter situation is extremely unlikely, as this means that a second ray connecting a different source-receiver pair would reflect at the same depth point.

In equation (12), the amplitude factor $\Lambda(M_R; \xi^*)$ is given by

$$\Lambda(M_R; \xi^*) = \frac{B(M_R; \xi^*)}{|\det \mathbf{H}_F|^{1/2}} \times \exp\left[-i\frac{\pi}{2}[1 - \mathrm{Sgn}\,(\mathbf{H}_F)/2]\right], \quad (14)$$

where $\mathbf{H}_F$ is the second-derivative (Hessian) matrix of $\tau_F(\xi)$ taken at ξ^*. This matrix is assumed to be nonsingular; i.e., $\det(\mathbf{H}_F) \neq 0$. Its signature $\mathrm{Sgn}\,(\mathbf{H}_F)$ is the number of positive eigenvalues minus the number of negative ones. Note that $\Lambda = \mathcal{A}R_c$ if the weight in equation (2) is chosen to be the true-amplitude weight (Schleicher et al., 1993).

To derive an approximate expression for the second term in equation (11), we take the derivative of equation (9) with respect to z. We observe that

$$\frac{\partial \hat{V}_1}{\partial z}(M_R; \omega) = \hat{W}(\omega)\frac{i\omega}{2\pi}\int\int_A d^2\xi \frac{\partial}{\partial z}[B(M; \xi)e^{i\omega\tau_F(M;\xi)}]\Big|_{M=M_R}$$

$$= \hat{W}(\omega)\frac{i\omega}{2\pi}\int\int_A d^2\xi \left[\frac{\partial B}{\partial z}(M; \xi)e^{i\omega\tau_F(M;\xi)} + B(M; \xi)(i\omega)\frac{\partial \tau_F}{\partial z}(M; \xi)e^{i\omega\tau_F(M;\xi)}\right]_{M=M_R}. \quad (15)$$

For high frequencies, the term of order ω^2 dominates as long as $\partial\tau_F/\partial z \neq 0$, so that we can write

$$\frac{\partial \hat{V}_1}{\partial z}(M_R; \omega) \simeq \hat{W}(\omega)\frac{(i\omega)^2}{2\pi} \times \int\int_A d^2\xi\, m(\xi)B(M_R; \xi)e^{i\omega\tau_F(M_R;\xi)}, \quad (16)$$

where we used the notation

$$m(\xi) = \frac{\partial \tau_F}{\partial z}(M_R; \xi). \quad (17)$$

The evaluation of integral (16) is readily performed in the same way as is done with integral (9), as we need to again determine its value at point M_R on the reflector. By application of the method of stationary phase, we obtain the asymptotic result

$$\frac{\partial \hat{V}_1}{\partial z}(M_R; \omega) \simeq i\omega m_0 \hat{W}(\omega)\Lambda(M_R; \xi^*), \quad (18)$$

where $\Lambda(M_R; \xi^*)$ is again given by equation (14). The symbol m_0 denotes the value of m at the stationary point; i.e., $m_0 = m(\xi^*) = \partial\tau_F/\partial z(M_R, \xi^*)$. Since the reflection time surface $\tau_R(\xi)$ does not depend on M and therefore not on z, we may also write

$$m_0 = \frac{\partial \tau_D}{\partial z}(M_R, \xi^*). \quad (19)$$

It remains to prove that the distorted migration output at M is indeed proportional to $W(m_0(z - z_0))$ and that m_0, as given by equation (19), is in agreement with the expression for $\Delta\tau/\Delta z$ given by formula (1).

For that purpose, we insert equations (12) and (18) into equation (11) to obtain

$$\hat{V}_1(M; \omega) \simeq [1 + i\omega m_0(z - z_0)]\hat{W}(\omega)\Lambda(M_R; \xi^*). \quad (20)$$

Back in the time domain, we have consequently

$$V_1(M, t) \simeq [W(t) + m_0(z - z_0)\dot{W}(t)]\Lambda(M_R; \xi^*). \quad (21)$$

Following equation (8), we now set $t = 0$ to obtain

$$V(M) = V_1(M, t = 0) \simeq [W(0) + m_0(z - z_0)\dot{W}(0)]\Lambda(M_R; \xi^*). \quad (22)$$

We finally note that, for small $|m_0(z - z_0)|$, we have in accordance with a first-order Taylor series expansion of $W(t)$ in the vicinity of $t = 0$

$$W(t = 0) + m_0(z - z_0)\dot{W}(t = 0) \simeq W(t = m_0(z - z_0)). \quad (23)$$

Hence, we find the desired expression

$$V(M) \simeq \Lambda(M_R, \xi^*)W(m_0(z - z_0)). \quad (24)$$

This result proves that at a point M vertically below a specular reflection point M_R, the output of a diffraction-stack migration is the distorted source wavelet with the same amplitude factor $\Lambda(M_R, \xi^*)$ as at the point M_R. The stretching factor m_0 is given by equation (19). Finally, we are now going to analyze equation (19) to prove that it indeed represents the same formula for the stretching factor as the one previously derived in a purely heuristical manner.

Geometrical interpretation

Using a point M that differs from M_R only in the z-coordinate (Figure 3a) and considering a source pulse $W(t)$, we showed that the diffraction-stack output at M is proportional to the "distorted pulse" $W(m_0(z - z_0))$, where the stretching factor

$$m_0 = \frac{\partial \tau_D}{\partial z}(M_R; \xi^*). \quad (25)$$

This factor turns out to have the simple geometrical meaning concealed in formula (1). To prove this, we carry out the differentiation of the diffraction traveltime function τ_D with respect to z; viz.,

$$m_0 = \frac{\partial \tau_D}{\partial z}(M_R; \xi^*) = \mathbf{n}_z \cdot \nabla_M \tau_D(M_R; \xi^*) = \mathbf{n}_z \cdot (\nabla_M \tau(S, M) + \nabla_M \tau(M, G))\Big|_{M_R}, \quad (26)$$

where $\tau(S, M)(\tau(M, G))$ is the traveltime along the ray branch from S to M (from M to G), and n_z is the unit vector in the z-direction. By the eikonal equation, the gradient of an eikonal function τ at a certain point equals the slowness vector of the ray at that point (Červený, 1987). Therefore, the latter expression is exactly the sum of the vertical components of the slowness vectors of the two ray branches at M_R. Since the modulus of the slowness vector at the point M_R is $1/v_{M_R}$, we arrive at

$$m_0 = \frac{1}{v_{M_R}}[\cos \Theta^-_{M_R} + \cos \Theta^+_{M_R}], \quad (27a)$$

where $\Theta^{\pm}_{M_R}$ is the acute angle that the incident/reflected ray branch makes with the vertical axis at M_R (Figure 3b). Equation (27a) proves that our heuristical argumentation led us indeed to the correct expression for the stretching factor m_0.

From Figure 3b, we observe that $\Theta_{M_R}^{\pm} = \Theta \mp \beta$, where Θ is the reflection angle and β is the local reflector dip in the plane of reflection; i.e., in the plane that is defined by the two slowness vectors of the ray branches at M_R. Equation (27a) can therefore be recast in the form

$$m_0 = \frac{2}{v_{M_R}} \cos \Theta \cos \beta. \qquad (27b)$$

We conclude from equation (27b) that, once the factor m_0 is known, it provides a relationship between the following three quantities: v_{M_R} (local velocity at M_R), Θ (reflection angle at M_R), and β (reflector dip at M_R). Hence, once two of these quantities are known, the other one can be computed.

As a result of equation (25), the stretching factor m_0 can be estimated once M_R and $\boldsymbol{\xi}^*$ are known, because in a Kirchhoff-type diffraction stack the traveltime surface $\tau_D(M; \boldsymbol{\xi})$ is computed for all subsurface points M and for all vector parameters $\boldsymbol{\xi}$. Both quantities M_R and $\boldsymbol{\xi}^*$ may then, for instance, be computed with a vector diffraction stack or modifications of it (Tygel et al., 1993). There is no need to identify reflections in the $(t, \boldsymbol{\xi})$ domain and to construct the envelopes of the isochrones. Alternatively, the parameter m_0 could be estimated from the data by comparing the length of the seismic source wavelets in the time and depth domains (i.e., the width L of the reflection time strip with the varying width of the depth-migrated strip).

We remark that for the considerations in this paper, the macro-velocity model is assumed to be represented by a continuous velocity function across the true location of the reflector. If this is not the case, the considerations of this paper remain completely unchanged for points M in the portion of the depth-migrated strip that lies above or below the reflector. All formulas are valid with the understanding that they are evaluated separately for points M above or below the interface. For example, in expressions (27) for m_0, the velocity v_{M_R} at point M_R is to be replaced by the velocity $v_{M_R}^-$ above or by $v_{M_R}^+$ below the reflector at M_R. The same applies to the angles $\Theta_{M_R}^-$ and $\Theta_{M_R}^+$.

SYNTHETIC EXAMPLE

To examine whether the derived formula for the wavelet's distortion in Kirchhoff-type depth migration is valid, we performed a simple 2-D synthetic example using a symmetrical Gabor wavelet (Gabor, 1946; Morlet et al., 1982) with a dominant frequency of 40 Hz. The earth model (see bottom left box in Figure 4) consists of two homogeneous layers separated by a horizontal interface at a depth of 0.6 km. The fairly shallow reflector was chosen to cover a large range of reflection angles. The P-wave velocity is 4 km/s in the upper layer, and 4.1 km/s in the lower one. A common-shot situation was simulated with the source position at 0 km, and 120 receivers were distributed equidistantly between 0 km and 3 km offset. The reflection angle varies from 0 to about 68 degrees. Figure 4 depicts the synthetic shot record where each trace has been normalized to its maximum. As the data were computed by ray-theoretical forward modeling, the wavelet length is identical for all traces. These data were migrated using the 2-D Kirchhoff-type diffraction-stack migration described by Hanitzsch et al. (1994). The normalized depth-migrated data are shown in Figure 5. The target zone of the migration was reduced to the illuminated part of the reflector. The pulse distortion is clearly visible. Note that only the depth range from 0.45 to 0.75 km is shown. Therefore, the pulse distortion effect looks much larger than it would be in a conventional seismic depth-migrated image. Figure 6 compares the wavelet length along the imaged

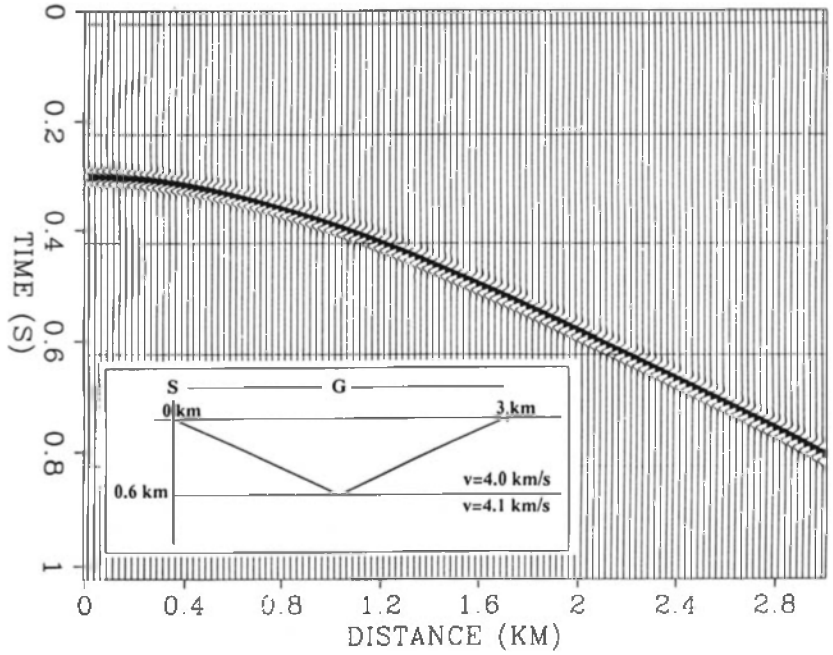

FIG. 4. Synthetic shot record data example. The seismic reflections are computed by ray theory for the model indicated in the bottom left box. The fairly shallow reflector was chosen to cover a large range of reflection angles.

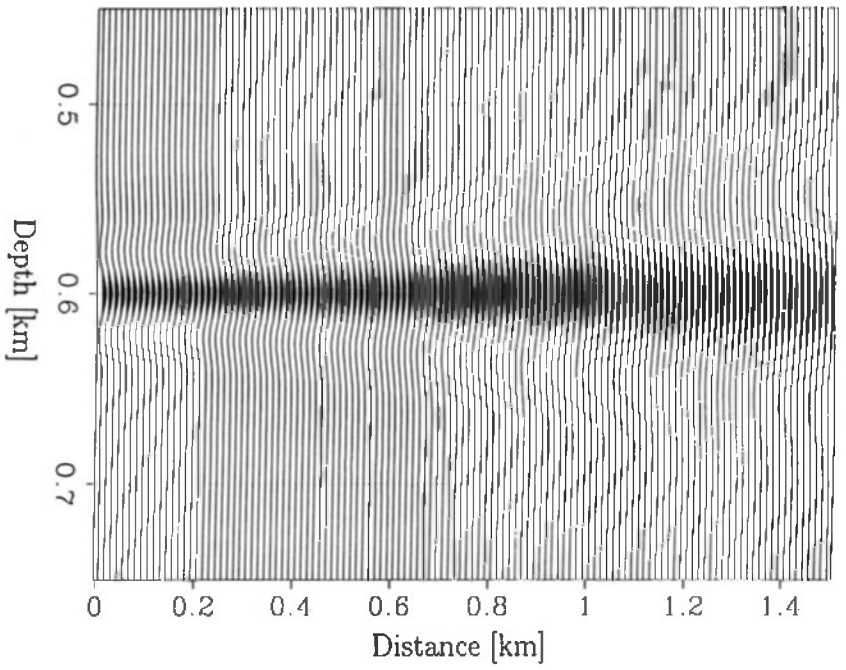

FIG. 5. Migrated data. The migration result is shown within the depth range from 0.45 km to 0.75 km and offset range 0 km to 1.5 km.

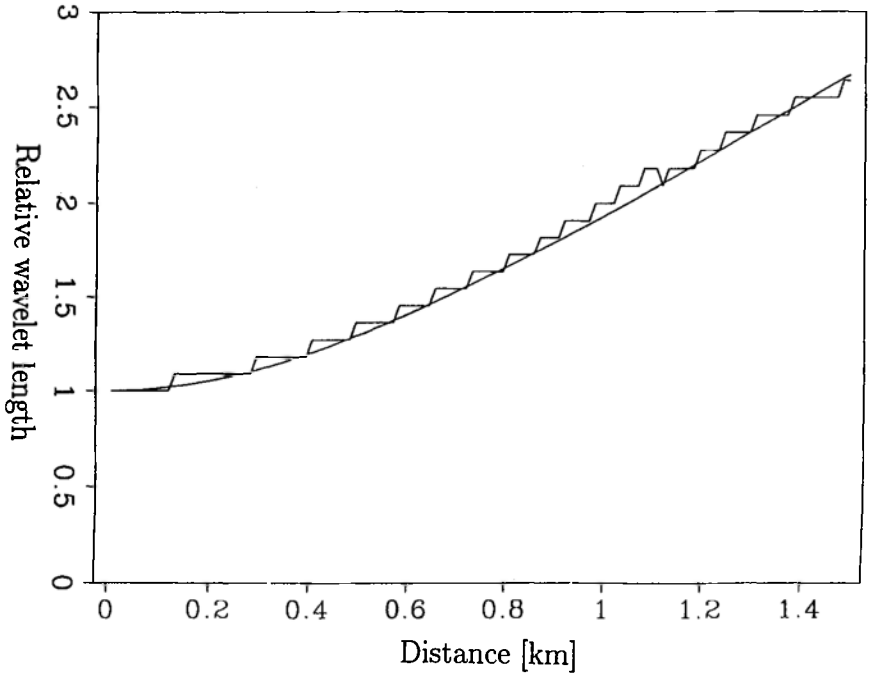

FIG. 6. Comparison between the wavelet length determined from the migrated reflector image of Figure 5 and the result predicted by the theory.

reflector, as obtained from the migrated image in Figure 5, with the theoretical value as predicted by formulas (27). Both curves coincide quite well. The steps in the picked curve are a result of sampling. We observe that in a distance of 1.5 km; i.e., for a reflection angle of about 68 degrees, the pulse is about 2.7 times longer than the zero-offset reflection pulse. For reflection angles less than 25 degrees, the pulse distortion is less than 10 percent and may be neglected. The situation does not change for a dipping reflector as can be seen from equation (27b). The effect decreases for synclinal structures, but it increases for anticlinal ones. Note that the pulse distortion decreases with increasing reflector depth as the range of reflection angles decreases.

CONCLUSIONS

It is a well-known fact that a depth migration using Kirchhoff-type diffraction stack results in distorted wavelets in depth irrespective of whether the macro-velocity model is right or wrong. In this paper, we have investigated this distortion both geometrically and mathematically. In both approaches, the same expression for the stretching factor was obtained. Since this factor depends only on the local velocity at the reflection point, the reflection angle, and the reflector dip, one of these quantities can be estimated from it, provided the other two are already known. We have also indicated how the distortion factor can be obtained directly from the seismic data. Either it can be determined without identifying reflections in the data [e.g., by a vector diffraction stack (Tygel et al., 1993) or by comparison of the estimated lengths of the migrated and unmigrated reflection wavelets]. The length of a wavelet can, of course, be determined from events observed in either the time or depth domains. The ratio of the so-determined wavelet lengths would also provide the distortion factor.

Having demonstrated how the length of a depth-migrated pulse varies with different raypaths, we have implicitly addressed the important question of vertical resolution. In the case of two closely spaced horizontal reflectors, we envision that situations may exist where the depth migration can resolve reflectors for short shot-receiver distances but not for long ones.

ACKNOWLEDGMENTS

We thank Sergei Goldin, Andrzei Hanyga, Milton Lopes, and Lucio Santos, for fruitful discussions and helpful comments and Martin Widmaier for his help when preparing the figures. Moreover, we thank Vlatislav Červený, Christian Hanitzsch, and Ivan Pšenčik for providing us with their program codes with which the numerical computations in this work were performed. Many thanks go also to the Associate Editor, Keh Pann, for his very constructive remarks, as well as to Douglas Hanson, Brian Sumner, and one unknown referee for their competent reviews.

The research of this paper has been supported in part by the National Council of Technology and Development (CNPq-Brazil), by a grant of CEPETRO/UNICAMP/PETROBRAS, by the Research Foundation of the State of São Paulo (FAPESP-Brazil), and by the Commission of the European Communities in the framework of the JOULE II Working Programme. The responsibility for the content remains with the authors. This is Karlsruhe University, Geophysical Institute Publication No. 605.

REFERENCES

Berkhout, A. J., 1984, Seismic resolution, a quantitative analysis of resolving power of acoustical echo techniques, Geophys. Press.

Bleistein, N., 1984, Mathematics of wave phenomena, Academic Press, Inc.

——— 1987, On the imaging of reflectors in the earth: Geophysics, **52**, 931–942.

Červený, V., 1987, Ray methods for three-dimensional seismic modeling, Norwegian Institute for Technology: Petroleum Industry Course.

Gabor, D., 1946, Theory of communication: J. IEEE, **93**, 429–441.

Hanitzsch, C., Schleicher, J., and Hubral, P., 1994, True-amplitude migration of 2-D synthetic data: Geophys. Prosp., **42**, 445–462.

Morlet, J., Arens, G., Fourgeau, E., and Giard, D., 1982, Wave propagation and sampling theory—Part II: Sampling theory and complex waves: Geophysics, **47**, 222–236.

Schleicher, J., Tygel, M., and Hubral, P., 1993, 3-D true-amplitude finite-offset migration: Geophysics, **58**, 1112–1126.

Tygel, M., Schleicher, J., Hubral, P., and Hanitzsch, C., 1993, Multiple weights in diffraction stack migration: Geophysics, **58**, 1820–1830.